DROP EVAPORATION BEHIND SHOCK WAVES IN A DRY FOAM

A. B. Britan and N. M. Kortsenshtein

UDC 533.552.529.5,533.6,011.72

1. Introduction. Questions of drop behavior behind shock waves in two-phase flows have been considered in [1-5]. For coarse drops the dynamics of breakup were considered in [1], while [2] dealt with the effect of interphase friction on velocity relaxation and [3] treated phase transformations. Shock wave structure was calculated in the most complete formulation in [4], with consideration of breakup, phase conversion, and liquid removal from the surface of large drops. The effect of problem parameters (wave intensity, mass content of drops, etc.) on relaxation zone structure was analyzed.

It is difficult to realize a homogeneous flow of a drop suspension in gas with controlled parameters in experiment. Therefore the majority of results has been obtained with an isolated large (~100 μ) drop or with a flow of regular structure with drop injection at a fixed frequency [5]. Information on shock wave propagation in finely dispersed fog-type media is important for a number of practical applications. In [6] a fog was produced by condensation of water from a mixture with nitrogen in a rarefaction wave within a shock tube. The ~10 μ drops thus formed were heated by a shock wave excited in the tube with some delay relative to the appearance of the fog.

In [7, 8] a finely dispersed medium was formed behind a shock wave front in a dry polyhedral foam with a mean density of ~2 kg/m^3. Frame-by-frame photography of the flow pattern and pressure recording permitted study of the dynamics of foam cell destruction and the process of drop formation. In [8] laser probing of a flow was used to measure the parameters and dynamics of drop velocity relaxation behind a shock wave front. In the present study, which is a continuation of [7, 8], we will consider features of the final stage of gas suspension flow, when the flows of gas and drops move with constant and identical velocities, and drop heating leads to their evaporation.

2. Medium Transparency and Gas Suspension Parameters. Shock tube construction and the laser probing method were described in detail in [8]. To fill the tube channel with a layer of foam of height $h \leqslant 2/3L$ (L = 1.44 m is the channel length) air at an overpressure of 0.03 MPa was bubbled through a volume of a 3% water solution of a surface-active substance (sodium alkyl sulfate). Foam cell size (0.3-1 cm) was regulated by controlling the air flow rate and the volume of solution on the bottom of the tube. After filling the channel with foam the liquid residue was drained through an orifice in the tube face [8]. Laser probing permitted continuous recording of the medium's transparency $F = J/J_0$, where J_0 is the initial radiation intensity, and J is the intensity of the radiation after transversing the flow. If the quantity J varies by the Bouguer law

$$dJ = -J_0 K_e dH,$$

the flow transparency in a channel of constant transverse dimension H for J_0 = const depends solely on the attenuation coefficient $K_e = K_a + K_s$ (where K_a and K_s are the absorption and scattering coefficients). In our case $K_a \ll K_s$ and medium transparency F is determined by scattering of radiation on drops [8]. It was shown in [9] that laser probing of a flow over two wavelengths permits evaluation of the dynamics of gas suspension parameters, which are related to F by the simple expression

$$F = \exp\left[-\frac{3}{2}(\bar{K}/D_{32})C_V H\right],$$

where $\bar{K}$ is the mean radiation scattering coefficient, which is practically independent of the form of the particle distribution over size; D_{32} is the mean or pre-breakoff drop diameter; C_V is the volume drop concentration (the volume occupied by drops per unit volume of gas suspension).

Moscow. Translated from Prikladnaya Mekhanika i Tekhnicheskaya Fizika, No. 4, pp. 32-38, July-August, 1993. Original article submitted April 25, 1992.

 0021-8944/93/3404-0480$12.50

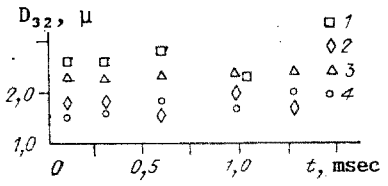

Fig. 1

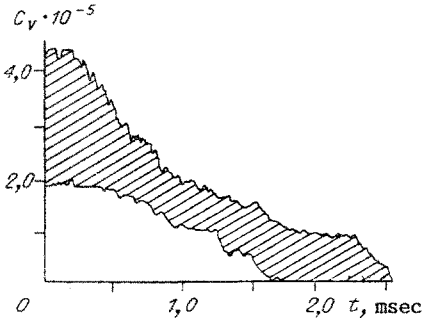

Fig. 2

For a monodispersed medium with constant number of drops n per unit volume (n = const) we write

$$C_V = \frac{\pi n}{6} D^3, \tag{2.1}$$

whence it is evident that a small (~10-15%) change in drop diameter D can lead to significant changes in C_V. Consequently, the dynamics of medium transparency in the present case are determined by the behavior of the volume concentration of drops in the flow.

Figures 1, 2 show the results of measurements of pre-breakoff drop diameter D_{32} and volume concentration of drops behind the shock wave front C_V, carried out by laser probing in [8]. Points 1-3 in Fig. 1 were obtained with a shock wave Mach number M = 1.32, and points 4 with M = 1.38. Foam layer heights were h = 30 and 60 cm (points 1, 2), 80 cm (3, 4). The horizontal axis of the figures shows time t relative to shock wave arrival at the measurement section. It is significant that in the various experiments the size of the drops formed was practically independent of t, M, and h. Since with increase in h the duration of drop stay within the flow increases, the effect of drop heating should be maximal in the experiments with h = 80 cm. The absence of such a dependence for the points of Fig. 1 shows that drop size is basically determined by the foam cell destruction processes. The uncertainty in D_{32} measurement, estimated at ±15% in [8], does not permit recording change in drop diameter in the flow due to evaporation.

The volume concentration measurements shown in Fig. 2 are more sensitive to droplet motion conditions in the flow. The size of the hatched region provides information on scattering in the initial concentration values C_V and the change in the slope $C_V(t)$ for experiments performed with fixed values h = 80 cm and M = 1.22. Equilibrium values of the flow parameters behind the shock wave front in this regime were: temperature T^0 = 363 K, pressure p^0 = 0.19 MPa, vapor pressure p_V^0 = 0.003 MPa. Table 1 presents values of C_V^0, D_{32} measured directly behind the wave front, and drop concentration n, calculated with Eq. (2.1) for the experiments of this series. We can see a general tendency to decrease in C_V with time, as well as the presence of a segment of constant C_V extending from 250 to 400 μsec. Over this time period the basic processes of foam cell destruction and drop speed relaxation in the flow are completed [7]. In all the oscillograms one can see a characteristic region with a less steep slope of the $C_V(t)$ curve, usually located at the end of the signal, which is related to arrival of the driver gas at the tube measurement section. Scattering of the laser radiation in this region is apparently controlled by the presence of hot drops which penetrate from the heated flow charge behind the shock wave [10]. The extent of the region in which the drops mix with the driver gas at M = 1.1-1.4 varied from 40 to 20 cm, while within an accuracy of ~10% the velocity of their motion coincided with the calculated flow velocity behind the shock wave [8].

The reason for the scattering in initial C_V and D_{32} values, as well as the differing slope of the $C_V(t)$ curves in experiments of a single series require special study. Within the present study an analysis was made of the tendency to decrease in drop volume concentration along the charge, common to all experiments, as well as an attempt to explain this effect by drop evaporation.

3. Computation Model, Considering Evaporation. In numerical modeling of interphase exchange in gas suspension flows the basic results and conclusions of [1-4] were obtained by comparison of theory with the experimental pressure profile behind the shock wave. The calculated pressure profile then depends to a significant degree on the value used for the drop

TABLE 1

Experiment number	$C_V \cdot 10^5$	D_{32}, μ	$n \cdot 10^{-13}$, m^{-3}
1	4.3	2.8	0.364
2	4.2	2.5	0.513
3	2.4	1.4	1.670
4	3.4	1.7	1.324
5	1.9	1.6	0.886
6	3.1	2.0	0.742
7	2.6	2.1	0,539

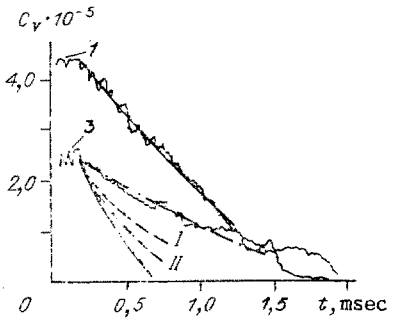

Fig. 3

aerodynamic resistance coefficient. Various dependences of this coefficient upon Reynolds number and other characteristics of the steady state flow over the drop are known, although data for nonsteady flow are extremely limited [5, 11]. This reduces the value of calculations performed in the full formulation, since the pressure profile in the relaxation zone is determined by velocity relaxation processes [12].

For the flow of a finely dispersed gas suspension the situation simplifies, since micron-size drops accelerate rapidly and the volume concentration C_V in the main part of the flow is determined by drop evaporation kinetics [6]. The calculation model can then neglect the initial stage of flow formation: foam collapse, formation and velocity relaxation of the drops, assuming that these processes end before evaporation begins. It is assumed that the gas, vapor, and drops move with a constant identical velocity, which, according to [8], can be calculated using the shock adiabat for air. The diameter of a drop of the monodispersed mixture D coincides with the measured value $D_{32} = 2r$. Given the condition that n = const over the entire volume of collapsed foam, the change in C_V should be related to the change in drop radius r:

$$\frac{dC_V}{dt} = 4\pi n r^2 \frac{dr}{dt}. \tag{3.1}$$

If the drop size changes only due to evaporation, then to calculate dr/dt we can use the Fuchs interpolation formula [13]

$$\frac{dr}{dt} = \frac{D_V \mu_V}{\rho_l RT}\left[p_V - p_V^s(T_d)\right]\left(\frac{r^2}{r+l} + \frac{D_V}{\alpha_C}\sqrt{\frac{2\pi\mu_V}{RT}}\right)^{-1}, \tag{3.2}$$

which is valid over a wide range of flow regimes from Knudsen ($r \ll \ell$) to continual ($r \gg \ell$). Here $\ell = 0.05\ \mu$ is the mean free path length; D_V is the diffusion coefficient, μ_V is the molecular mass, p_V is the partial pressure, $p_V^s(T_d)$ is the saturation vapor pressure at the drop temperature T_d, ρ_ℓ is the density of water, α_C is the condensation (evaporation) coefficient. The subscripts V and d refer to parameters of the vapor and drops, respectively.

Due to evaporation the drop temperature changes by a law

$$c_{pl} m \frac{dT_d}{dt} = B\frac{dm}{dt} + 4\pi r^2 \alpha (T - T_d), \tag{3.3}$$

where m is the drop mass, B is the specific heat of evaporation, $c_{p\ell}$ is the specific heat of the drop material, α is the heat liberation coefficient. Using the expressions for the Nusselt number, from Eq. (3.3) we obtain

$$\frac{dT_d}{dt} = \frac{3B}{c_{pl} r^2}\left[r\frac{dr}{dt} + \frac{\mathrm{Nu}\lambda_g}{2\rho_l B}(T - T_d)\right]. \tag{3.4}$$

Here λ_g is the thermal conductivity coefficient of the gaseous phase; $\mathrm{Nu} = \alpha 2r/\lambda_g$.

Together with the temperature in the flow, the partial vapor pressure can also change:

$$\frac{dp_V}{dt} = -\frac{\rho_l RT}{\mu_V}\frac{dC_V}{dt}. \tag{3.5}$$

Yet drop evaporation does not affect the net pressure in the flow, since $p_V/p \sim 10^{-2}$.

The system of equations (3.2)-(3.5) is closed and can be integrated numerically by the Runge–Kutta method to find the function $C_V(t)$. For initial conditions we use the values T^0, p^0, p_V^0, as well as the quantities C_V^0 and D_{32} measured directly behind the front.

4. Evaluation of Results. For comparison with calculation considering the process of drop evaporation typical $C_V(t)$ curves obtained in experiments 1 and 3 from the table were used (Fig. 3). The solid curves of Fig. 3 correspond to the evaporation coefficient α_C = 0.036 [13] usual for water drops. Agreement between theory and experiment is found only for experiment 1. We note that experiments 1 and 2 differed from the remaining results of this series in the maximal slope of the $C_V(t)$ curves and elevated values of D_{32} and C_V (see Table 1). In experiments 3-7 there was a stable correlation between a reduction by approximately a factor of two in D_{32} and C_V and a decrease in the slope of the $C_V(t)$ curves. For experiment 3, demonstrated in Fig. 3, agreement with calculation can be achieved only at α_C = 0.0036 (dash-dot curve). Decrease in the coefficient α_C implies that the theory proposes a significant, almost tenfold, reduction in water evaporation rate. In experiment such an effect might be related, for example, to an elevated concentration of surface-active substance in the foam composition for experiments 3-7. The excess material might collect on the channel walls and dissolve in the foam-forming solution as the channel is filled with foam. It is known that the presence of surface-active material, which was not considered in the calculations, stabilizes the composition of the drops formed, since it reduces the liquid surface tension. The drop distribution function then becomes more elongated, while the mean drop size decreases [10], which agrees with the data of experiments 3-7 shown in Table 1. The presence of excess surface-active substance should also decrease the evaporation rate due to decrease in the curvature of the saturation curve.

Another explanation of the effect noted might be found in the simplifications of the physical concepts used in deriving the basic equations. The first of these is related to the monodispersion approximation, so estimates were made of the possibility of existence in the flow of drops of two characteristic sizes – a so-called bidispersed gas suspension. In that case the measured values D_{32} and C_V can be defined as

$$D_{32} = \frac{n_1 D_1^3 + n_2 D_2^3}{n_1 D_1^2 + n_2 D_2^2}, \tag{4.1}$$

$$C_V = \frac{\pi}{6}(n_1 D_1^3 + n_2 D_2^3), \tag{4.2}$$

where $n_{1,2}$ and $D_{1,2}$ are the number of drops per unit volume and the drop diameter for each fraction. Introducing limitations on drop size

$$D_1 = D_{32}/a, \quad a \geqslant 1; \tag{4.3}$$

$$D_2 = D_{32}/b, \quad b \leqslant 1, \tag{4.4}$$

the system (4.1), (4.2) is completed and all parameters of the bidispersed gas suspension can be found in terms of a and b:

$$n_1 = \frac{c(1-b)}{a-b}\left(\frac{a}{D_{32}}\right)^3; \tag{4.5}$$

$$n_2 = \frac{c(a-1)}{a-b}\left(\frac{b}{D_{32}}\right)^3. \tag{4.6}$$

Here $c = 6C_V/\pi$. With consideration of Eqs. (4.1)-(4.6) the relationship between the parameters for the mono- and bidispersed approximations has the form

$$\frac{D_1}{D} = \frac{1}{a}, \quad \frac{D_2}{D} = \frac{1}{b}, \quad \frac{n_1}{n} = a^3\left(\frac{1-b}{a-b}\right), \quad \frac{n_2}{n} = b^3\left(\frac{a-1}{a-b}\right).$$

We write Eq. (3.1) for the bidispersed mixture as

$$\left(\frac{dC_V}{dt}\right)_{bD} = 4\pi\left(n_1 r_1^2 \frac{dr_1}{dt} + n_2 r_2^2 \frac{dr_2}{dt}\right). \tag{4.7}$$

Dividing Eq. (4.7) by Eq. (3.1) we obtain

$$\xi \equiv \frac{(dC_V/dt)_{bD}}{dC_V/dt} = \frac{n_1}{n}\left(\frac{r_1}{r}\right)^2 \frac{\dot{r}_1}{\dot{r}} + \frac{n_2}{n}\left(\frac{r_2}{r}\right)^2 \frac{\dot{r}_2}{\dot{r}}, \qquad \dot{r} \equiv \frac{dr}{dt}.$$

Note that directly behind the shock front the flow parameters correspond to the calculated adiabat for air, while C_V and D_{32} take on the initial values for the drops formed. The quantity ξ then also depends on a and b:

$$\xi = \frac{1+\Delta}{a-b}\left[\frac{a^2(1-b)}{1+a\Delta} + \frac{b^2(a-1)}{1+b\Delta}\right] \qquad \left(\Delta = \frac{2\delta}{D_{32}}, \ \delta = \frac{D_V}{\alpha_C}\sqrt{\frac{2\pi\mu_V}{RT}}\right).$$

Together with the limitations $a \geqslant 1$ and $0 \leqslant b \leqslant 1$, which are obvious, we introduce an additional condition on the total volume of drops of the large and small fractions formed during foam collapse:

$$\frac{n_1 D_1^3}{n_2 D_2^3} \equiv \gamma = \frac{1-b}{a-1}.$$

Assuming that the fine drops are formed by destruction of films, and the coarse ones, by destruction of channels of the foam cell, we can make use of the data of [14], which indicate that from 1 to 20% of all the liquid in the foam is contained in films. Results of ξ calculations performed for values γ = 0.01-0.2 differ from unity by not more than 2-3%. It follows from this that initial bidispersion of the medium could not make a significant change in the calculated $C_V(t)$ dependences shown by the solid lines of Fig. 3.

We will consider the effect of another simplification of the calculation model, the absence of drop collisions in the flow, in the monodispersed approximation. Without discussing the reasons which produce drop collisions, we will note that such collisions can only result in merger, since fractionation of micron size drops is not probable. Coagulation decreases the number of drops, but increases their size while maintaining the net drop volume C_V. This should result in decrease in total drop surface, decrease in evaporation rate, and flatter character of the $C_V(t)$ curve. In the presence of coagulation the numerical drop concentration is defined by the expression

$$dn/dt = -kn^2,$$

where $k = \pi D^2 v$, v is the relative velocity of the drops upon collision. Together with evaporation, coagulation affects drop size, so we write

$$\frac{dr}{dt} = \left(\frac{dr}{dt}\right)_0 + \left(\frac{dr}{dt}\right)_c, \tag{4.8}$$

where the first term on the right is defined by Eq. (3.2) and the second, by the expression

$$\left(\frac{dr}{dt}\right)_c = -\frac{r}{3n}\frac{dn}{dt}.$$

Numerical integration of system (3.1), (3.4), (4.8) was carried out for v = 2 and 20 m/sec, whose values are 1 and 10% of the flow velocity, respectively. Lines I and II of Fig. 3 correspond to the first and second of these variants. Consideration of coagulation does in fact decrease the slope of the calculated $C_V(t)$ curves, with the effect being most intense for the experiments with elevated initial drop concentration. For small n the effect of coagulation is insignificant and the dashed curve for experiment 1 in Fig. 3 practically coincides with the solid line. Since consideration of coagulation does not allow agreement of the calculated curves with experiment for $C_V(t)$, the simplification of the model by neglect of this effect can be considered justifiable.

Results of the calculations performed and comparison with experimental data permit the following conclusions.

1. Under the conditions considered the process of dry foam destruction behind a shock wave ends in intense evaporation of drops in the flow. Due to evaporation the volume concentration of drops can be reduced to almost half over the course of ~1 msec. With drop prebreakoff diameter measurement to an accuracy of ±15% no effect of evaporation on that parameter was noted.

2. For fixed initial conditions there is a significant scattering in experimental parameters of the drops and evaporation rate. Special experiments with controlled change of surface-active substance concentration in the foam will be required to clarify the causes of this scattering.

3. For correct description of experiment by the calculation model considering drop evaporation, the experimental $C_V(t)$ dependence can be used to determine the dynamics of drop temperature in the flow. From Eq. (3.2) we write

$$p_V^s(T_d) = p_V^0 + (1-\eta^3)\frac{D_V}{\varepsilon} - \frac{D_{32}(0.5\eta D_{32} + \delta)}{6\varepsilon\eta^2 C_V^0}\frac{dC_V}{dt}, \tag{4.9}$$

where $\eta = (C_V/C_V^0)^{1/3}$, $\varepsilon = D_V\mu_V/(\rho_\ell RT^0)$, the subscript zero corresponds to parameters in the initial stage of the evaporation process. The parameters D_{32}, C_V, C_V^0, dC_V/dt on the right

side of Eq. (4.9) are known from experiment, while p_V^0, ε can be found by calculation with the shock adiabat equations for a given value of Mach number for the discontinuity. Knowing the elasticity curve for the drop material, from the value of p_V^S we find the drop temperature T_d.

The authors express their gratitude to I. N. Zinovik for his assistance in the study.

LITERATURE CITED

1. T. R. Amanbaev and A. I. Ivandaev, "Shock wave structure in two-phase mixtures of gas with liquid drops," Prikl. Mekh. Tekh. Fiz., No. 2 (1988).
2. A. I. Ivandaev, A. G. Kutushev, and R. I. Nigmatulin, "Gas dynamics of multiphase media," in: Achievements in Science and Technology, Mechanics of Liquids and Gases [in Russian], Vol. 16, VINITI, Moscow (1981).
3. R. I. Nigmatulin, "Hydromechanics equations and compaction waves in two-velocity two-temperature continuous media in the presence of phase conversions," Izv. Akad. Nauk SSSR, Mekh. Zhidk. Gaza, No. 5 (1967).
4. T. R. Amanbaev and A. I. Ivandaev, "Effect of drop breakup on shock wave structure in gas-drop mixtures," Prikl. Mekh. Tekh. Fiz., No. 3 (1988).
5. A. Ranger and J. Nicholls, "Aerodynamic scattering of liquid drop," AIAA J., 7, No. 2 (1969).
6. H. W. J. Goossens, M. J. C. M. Bercelmans, and M. E. H. van Dongen, "Experimental investigation of weak shock waves propagating in a fog," 15th Intern. Symp. on Shock Waves and Shock Tubes, Berkeley, CA, 1985: Proceedings, Stanford (1986).
7. A. B. Britan, I. N. Zinovik, and V. A. Levin, "Foam destruction by shock waves," Fiz. Goreniya Vzryva, No. 5 (1992).
8. A. B. Britan, I. N. Zinovik, and V. A. Levin, "Measurement of gas suspension parameters behind a shock wave in foam," Izv. Russk. Akad. Nauk, Mekh. Zhidk. Gaza, No. 2 (1993).
9. A. G. Golubev and V. I. Yagodkin, "Optical methods of aerosol measurement," Tr. TsIAM, No. 828 (1978).
10. G. A. Saltanov, Nonequilibrium and Nonsteady Processes in Gas Dynamics [in Russian], Nauka, Moscow (1979).
11. A. A. Borisov, B. E. Gel'fand, M. S. Natanzon, and O. M. Kossov, "Drop breakup regimes and criteria for their existence," Inzh. Fiz. Zh., 40, No. 1 (1981).
12. E. Outa, T. Tajima, and S. Suzukin, "Cross section concentration of particles during shock process propagating through a gas-particle mixture in a shock tube," in: Shock Tubes and Waves: Proc. 14th Intern. Symp. Shock Tubes and Shock Waves, University of Sydney, Australia, 1983, Sydney (1983).
13. L. E. Sternin, Fundamentals of Gas Dynamics of Two-Phase Flows in Nozzles [in Russian], Mashinostroenie, Moscow (1974).
14. K. B. Kan, Capillary Foam Hydrodynamics [in Russian], Nauka, Novosibirsk (1989).